Journal of Power Sources 219 (2012) 258–262

Contents lists available at SciVerse ScienceDirect

Journal of Power Sources

journal homepage: www.elsevier.com/locate/jpowsour

Multiwalled carbon nanotubes supported palladium–phosphorus nanoparticles for ethanol electrooxidation in alkaline solution

Ke Wu [a], Xinbiao Mao [b], Yan Liang [a], Yu Chen [a,*], Yawen Tang [a], Yiming Zhou [a], Jun Lin [a,*], Chunan Ma [b], Tianhong Lu [a]

[a] Jiangsu Key Laboratory of New Power Batteries, College of Chemistry and Materials Science, Nanjing Normal University, 1# Wenyuan Road, Nanjing 210046, PR China
[b] State Key Laboratory Breeding Base of Green Chemistry-Synthesis Technology, Zhejiang University of Technology, 18# Chaowang Road, Hangzhou 310014, PR China

HIGHLIGHTS

- Pd–P/MWCNTs is synthesized by homogeneous precipitation–reduction reaction method.
- Ultrafine Pd–P nanoparticles are highly dispersed on MWCNTs surface.
- Pd–P/MWCNTs shows excellent electrocatalytic activity for ethanol oxidation.

ARTICLE INFO

Article history:
Received 9 April 2012
Received in revised form
17 July 2012
Accepted 19 July 2012
Available online 27 July 2012

Keywords:
Carbon nanotubes
Palladium–phosphorus nanoparticles
Catalyst
Ethanol electrooxidation
Electrocatalytic activity

ABSTRACT

Multiwalled carbon nanotubes (MWCNTs) supported palladium-phosphorus nanoparticles (Pd–P/MWCNTs) catalyst is synthesized by homogeneous precipitation–reduction reaction method using hypohosphite as reducing agent. X-ray photoelectron spectroscopy (XPS) and X-ray diffraction (XRD) analysis confirm that some P has entered into the crystal lattice of Pd and thus the Pd–P alloy is formed. Transmission electron microscopy (TEM) images reveal that Pd–P nanoparticles are uniformly dispersed on MWCNTs and the average particle size of Pd–P/MWCNTs catalyst is very similar to that of Pd/MWCNTs catalyst prepared by using $NaBH_4$ as reducing agent. Cyclic voltammetric and chronoamperometric experiments show that the electrocatalytic activity and long-term operation stability of Pd–P/MWCNTs catalyst are better than that of Pd/MWCNTs catalyst for ethanol electrooxidation in alkaline media, indicating that the addition of P in Pd nanoparticles can promote the electrocatalytic activity and stability of Pd catalyst for ethanol electrooxidation.

1. Introduction

Direct ethanol fuel cells (DEFCs) have attracted more and more attention as a new generation of environment friendly power source due to its high energy density, low pollutant emission, low operating temperature, and ready availability and low toxicity of ethanol fuel. Recently, palladium (Pd), which is cheaper and more abundant than platinum (Pt), has been recognized as an effective catalyst for ethanol electrooxidation in alkaline solution [1]. However, there are still many difficulties associated with ethanol electrooxidation. For example, the complete oxidation of ethanol to CO_2 involves 12 electrons transfer and the scission of a C–C bond, which demands high activation energy to be overcome. Meanwhile, some intermediates (mainly CO and –CHO) produced during the oxidation reaction poison the anode catalyst and in turn reduce the catalytic efficiency [2]. Thus, the activity and stability of Pd catalyst are still in need of improvement.

Till now, various Pd-based binary alloy catalysts for ethanol electrooxidation, such as Pd–Ag [3], Pd–Sn [4–6], Pd–Ni [7,8], Pd–Au [9,10], Pd–Ru [11,12], and Pd–Pb [13], etc., have been developed successfully. However, ethanol electrooxidation on palladium-nonmetal binary catalyst is seldom reported. Meanwhile, our previous investigations demonstrate the phosphorus (P) doping can effectively improve the electrocatalytic activity of Pd catalyst for formic acid electrooxdiation due to electronic effect and ligand effect [14,15]. In this work, both multiwalled carbon nanotubes (MWCNTs) supported palladium nanoparticles (Pd/MWCNTs) and palladium-phosphorus nanoparticles (Pd–P/MWCNTs) catalysts with similar particle sizes are synthesized by homogeneous precipitation–reduction reaction method (i.e., $PdCl_2 \rightarrow PdO{\cdot}H_2O \rightarrow Pd^0$ reaction path) [16]. The as-prepared Pd–P/MWCNTs catalyst shows better electrochemical activity

* Corresponding authors. Tel.: +86 25 85891651; fax: +86 25 83243286.
E-mail addresses: ndchenyu@yahoo.cn (Y. Chen), linjun@njnu.edu.cn (J. Lin).

0378-7753/$ – see front matter © 2012 Elsevier B.V. All rights reserved.
http://dx.doi.org/10.1016/j.jpowsour.2012.07.059

and stability for ethanol electrooxidation than Pd/MWCNTs catalyst, indicating phosphorus doping effectively improve the electrocatalytic activity of Pd catalyst for ethanol electrooxdiation.

2. Experimental

2.1. Chemicals

Multiwalled carbon nanotubes (MWCNTs) (>95% purity; outer diameter 35 ~ 60 nm; inner diameter 25 ~ 40 nm; length 5 ~ 10 μm) used in this study were purchased from Chengdu Organic Chemicals Co., Ltd., Chinese Academy of Sciences. Naphthalen-1-ylmethylphosphonic acid (NYPA, shown in Scheme 1) was gifted by Dr. Pengfei Wang at Nanjing University. All other reagents were of analytical grade and used without further purification.

2.2. Synthesis of catalysts

The water-soluble phosphonate functionalized MWCNTs were synthesized by the π-π stacking interaction between MWCNTs and NYPA [17], which could effectively anchor $PdO{\cdot}H_2O$ nanoparticles to MWCNTs surface by the interaction between $-PO_3H_2$ groups and $PdO{\cdot}H_2O$ nanoparticles [18]. As described by Scheme 1, Pd–P/MWCNTs catalyst was prepared as follows: 3.0 mL of 0.045 M $PdCl_2$ solution and 60.0 mg of phosphonate functionalized MWCNTs were added into 27.0 mL water, and the suspension was ultrasonicated for 30 min. After adjusting solution pH to 5.5, the mixture was kept at 40 °C for 3 h to generate $PdO{\cdot}H_2O$/MWCNTs nanocomposites via hydrolyzation reaction of $PdCl_2$. Subsequently, 5 mL of 0.54 M NaH_2PO_2 solution was added into the suspension and then stirred for an additional 60 min. After filtration and dryness, Pd–P/MWCNTs catalyst was obtained. For comparison, MWCNTs supported palladium nanoparticles (Pd/MWCNTs) catalyst was also prepared by using $NaBH_4$ as reductant under the same preparation conditions.

2.3. Characterization of catalysts

Electrochemical measurements were performed in a conventional three-electrode electrochemical cell by using a CHI 660C electrochemical analyzer. A Pt plate auxiliary electrode and a saturated calomel reference electrode (SCE) were used. All potentials in this study were reported with respect to the SCE. For preparation of working electrode, typical process followed the previous procedure reported [19]. The specific loading of Pd metal on the electrode surface was about 28 μg cm^{-2}. Electrochemical measurements for ethanol electrooxidation were carried out in a mixed solution of 1 M KOH + 1 M CH_3CH_2OH. N_2 was bubbled through the solution for 20 min to remove the dissolved O_2 prior to the electrochemical measurements. CO-stripping voltammetry measurements were preformed according to previous procedure reported [19,20]. All electrochemical measurements were carried out at 30 ± 1 °C.

Metal loading in catalyst was accurately determined with a Leeman inductively coupled plasma atomic emission spectrometry (ICP-AES). XRD measurements were performed with Model D/max-rC diffractometer. The morphology and particle size of catalysts were investigated using a JEOL JEM-2010 transmission electron microscopy (TEM). X-ray photoelectron spectroscopy (XPS) measurements were carried out on a Thermo VG Scientific ESCALAB 250 spectrometer.

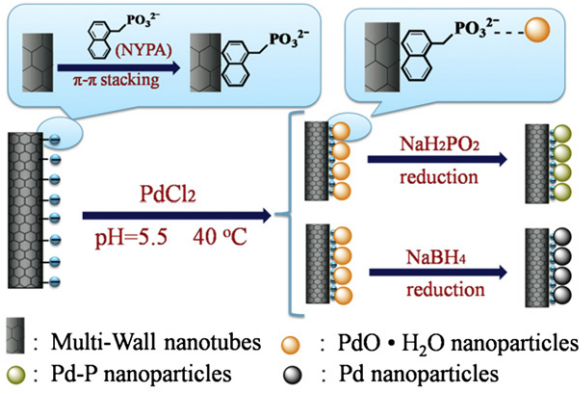

Scheme 1. Illustration of synthesis procedure of Pd/MWCNTs and Pd–P/MWCNTs catalysts.

3. Results and discussion

3.1. Physicochemical characterization of catalysts

Pd–P/MWCNTs and Pd/MWCNTs catalysts were synthesized using the improved homogeneous precipitation–reduction reaction method (i.e., $PdCl_2 \rightarrow PdO{\cdot}H_2O \rightarrow Pd^0$ reaction path) reported previously by us [16], as illustrated in Scheme 1. After adjusting pH value of $PdCl_2$ solution to 5.5, the resulting $PdCl_2$ solution (pH = 5.5) was heated to slowly generate $PdO{\cdot}H_2O$ nanoparticles. Then, the formed $PdO{\cdot}H_2O$ nanoparticles was reduced to obtain Pd^0 nanoparticles by using appropriate reduction reagent. Due to the strong reduction capacity of hypohosphite ($E = -0.504\ V + 0.06\ pH$) in acidic solution [21], hypohosphite can reduce intermediate $PdO{\cdot}H_2O$ nanoparticles to generate metallic Pd nanoparticles (Eq. (1)). ICP-AES analysis shows Pd–P/MWCNTs catalyst contains about 28.8 wt.% metal Pd, in accordance with Pd/MWCNTs catalyst (29.2 wt.%). In hypohosphite-metal salt system, the elemental phosphorus generated via hydrogenous free radical (Eq. (2)) and/or hydrogenous radical anion (Eq. (3)) mechanisms can react with metal (M) to form M-P alloy (Eq. (4)) [21–26]. As expected, ICP-AES analysis indicates the atomic ratio of Pd and P in the Pd–P/MWCNTs catalyst is 100:12, illustrating that phosphorus element is successfully introduced into Pd nanoparticles.

$$PdO{\cdot}H_2O + H_2PO_2^- \rightarrow Pd + H_2PO_3^- + H_2O \quad (1)$$

$$H_2PO_2^- + H^+ + H \rightarrow 2H_2O + P \quad (2)$$

$$H_2PO_2^- + 2H^+ + H^- \rightarrow 2H_2O + 1/2H_2 + P \quad (3)$$

$$nM + P \rightarrow M_nP \quad (4)$$

Fig. 1 shows XPS spectra of catalysts in P_{2p} and Pd_{3d} region. In the P_{2p} spectrum of Pd–P/MWCNTs catalyst, P_{2p} peaks at 130.4 and 134.3 eV are assigned to elemental state phosphorus (P^0) interacting with palladium and oxidized phosphorus (P^v), respectively [14]. In the previous reports, Pd–P and Pt-P catalysts were successfully prepared by using hypohosphite as reducing agent in weak alkaline conditions [27–31]. However, elemental state phosphorus (P^0) could not been observed. Thus, we presume that the low solution pH may facilitate the generation of elemental state phosphorus (P^0). The Pd_{3d} signal of Pd/MWCNTs catalyst is fitted to two pairs of doubles: $Pd_{3d3/2}$ (340.9 eV), $Pd_{3d5/2}$ (335.7 eV) and $Pd_{3d3/2}$ (342.9 eV), $Pd_{3d5/2}$ (337.7 eV), which can be assigned to Pd^0 and $Pd^{II}O$ species, respectively. For Pd–P/MWCNTs catalyst, the binding energies of Pd^0 and $Pd^{II}O$ species positively shift ca. 0.15 eV compared to Pd/MWCNTs catalyst. The positive shift of binding energies is attributed to Pd–P interaction [14], which reflects the

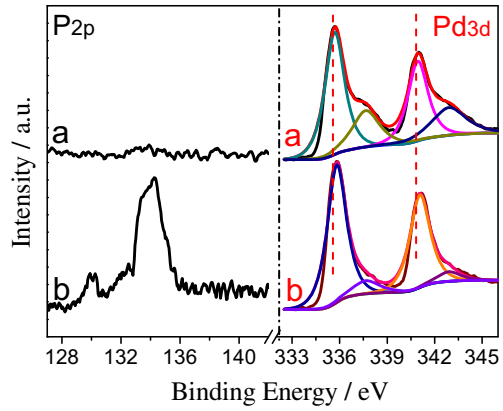

Fig. 1. XPS spectra of (a) Pd/MWCNTs and (b) Pd–P/MWCNTs catalysts.

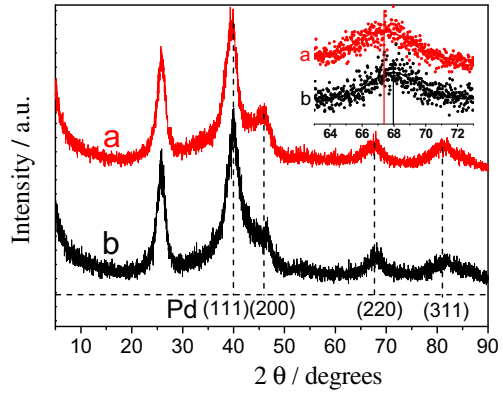

Fig. 2. XRD patterns of (a) Pd/MWCNTs and (b) Pd–P/MWCNTs catalysts.

downshift of d-band center of Pd atom in Pd–P nanoparicles [32–34], and consequently results in the decrease in interaction strength of the various adsorbates to Pd surface [35–39]. As observed, Pd–P/MWCNTs catalyst possess relatively less amount of oxide state ($Pd^{II}O$, 12.8%) than Pd/MWCNTs catalyst ($Pd^{II}O$, 26.2%), confirming that Pd–P/MWCNTs catalyst has a weaker oxophilicity than Pd/MWCNTs catalyst due to the downshift of d-band center of Pd atoms in Pd–P/MWCNTs.

The phase and purity of as-prepared products were determined by XRD (Fig. 2). Both Pd/MWCNTs and Pd–P/MWCNTs catalysts exhibit diffraction peaks of (111), (200), (220), (311), and (222) planes corresponding to a face centered cubic crystal structure (JCPDS 05-0681). A careful survey of Pd(220) peak reveals that diffraction peaks of Pd–P/MWCNTs catalyst are shifted to higher 2θ value compared to Pd/MWCNTs catalyst (Insert in Fig. 2), reflecting the lattice contraction due to the partial substitution of Pd by P [40–44]. In order to avoid disturbance of the diffraction peak of the carbon support, the average size of catalyst is calculated from the half peak width of the Pd(220) peak according to Scherrer equation [45]. The average particle sizes of Pd/MWCNTs and Pd–P/MWCNTs catalysts are calculated to be 3.3 and 3.4 nm, respectively.

Fig. 3 shows typical TEM images of catalysts. As observed, both Pd nanoparticles and Pd–P nanoparticles are highly dispersed on MWCNTs. Size distribution histograms show the average particle sizes of Pd/MWCNTs and Pd–P/MWCNTs are 3.6 and 3.5 nm, respectively, in good agreement with the values obtained from XRD. In our present work, all spectroscopic characterizations show particle size, morphology and structure of both catalysts are very similar, which can effectively clarify the effect of phosphorus doping on electrocatalytic activity of Pd catalyst for ethanol electrooxidation.

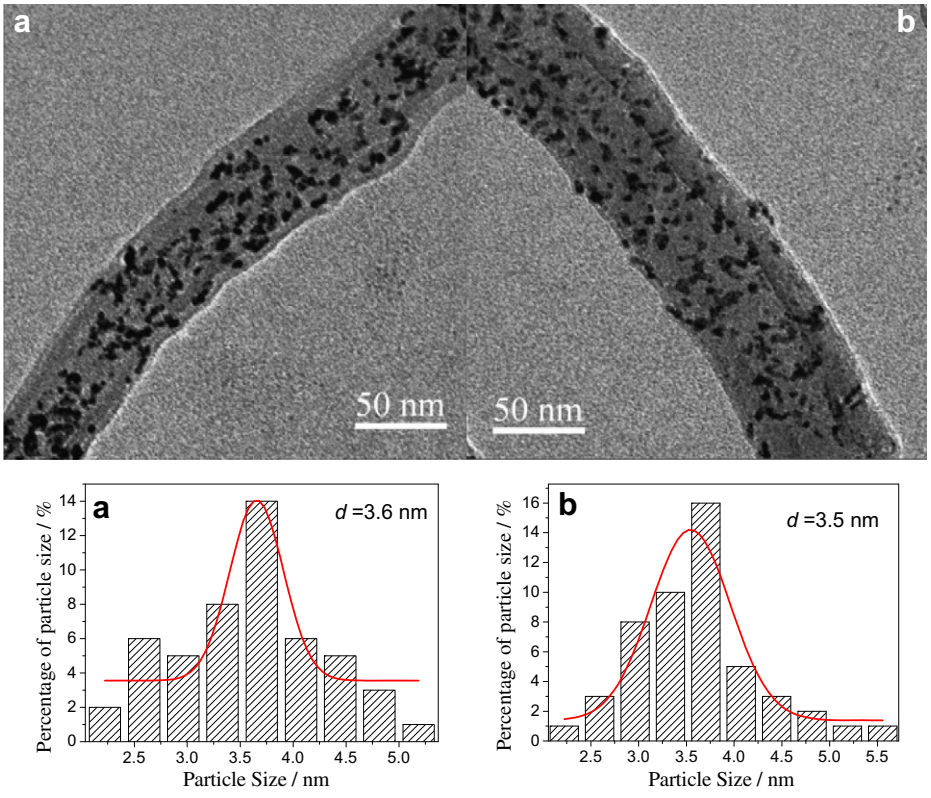

Fig. 3. TEM images and corresponding size distribution histograms of (a) Pd/MWCNTs and (b) Pd–P/MWCNTs catalysts.

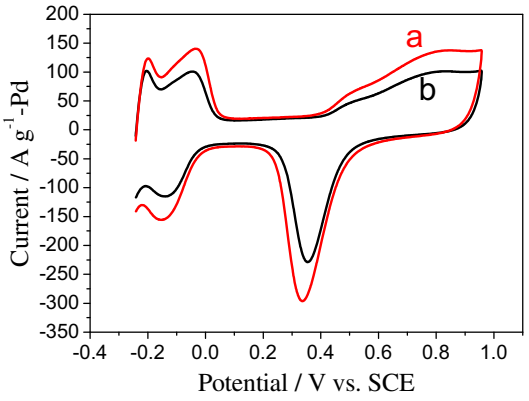

Fig. 4. Cyclic voltammograms of (a) Pd/MWCNTs and (b) Pd–P/MWCNTs catalysts in N_2-saturated 0.5 M H_2SO_4 solutions at 50 mV s^{-1}.

3.2. Electrocatalytic activity of catalysts for CH_3CH_2OH electrooxidation

Fig. 4 shows cyclic voltammograms of Pd–P/MWCNTs and Pd/MWCNTs catalysts in N_2-saturated 0.5 M H_2SO_4 solutions at 50 mV s^{-1}. As observed, the reduction peak potential of Pd oxide at Pd–P/MWCNTs catalyst shifts positively ca. 20 mV compared to Pd/MWCNTs catalyst, indicating that Pd–P/MWCNTs catalyst has the weaker oxophilicity than Pd/MWCNTs catalyst (i.e., Pd–P/MWCNTs catalyst has the lower hydroxyl surface coverage than Pd/MWCNTs catalyst) [42,46,47], in good agreement with the result of XPS measurement. Since adsorbed hydroxyl species inhibit ethanol oxidation, the lower hydroxyl surface coverage on Pd–P/MWCNTs may facilitate the ethanol oxidation kinetics.

Fig. 5 shows the CO-stripping voltammograms of Pd–P/MWCNTs and Pd/MWCNTs catalysts. The electrochemically active surface area (ECASA) of Pd–P/MWCNTs and Pd/MWCNTs catalysts can be calculated from the area of the oxidation peak of CO_{ad} through the following equation.

$$\text{ECASA} = Q/mC \quad (5)$$

where Q is the charge quantity for CO desorption electrooxidation, m is the mass of palladium on the electrode surface, and C is the oxidation charge/cm^2 of a monolayer CO on Pd surface (here, it is 420 μC cm^{-2}) [48]. Although particle sizes of both catalysts are very similar, the electrochemically active surface area of Pd–P/MWCNTs (59.6 g^{-1} m^2) is much lower than that of Pd/MWCNTs (108.2 g^{-1} m^2). In addition, it is observed that the oxidation peak potential of CO_{ad} at Pd–P/MWCNTs catalyst shifts negatively ca. 40 mV compared to Pd/MWCNTs catalyst. The above results illustrate that P doping can decrease the adsorption strength and amount of CO_{ad}, which facilitates the rate of the ethanol electrooxidation and enhances the anti-poisoning capability of catalyst.

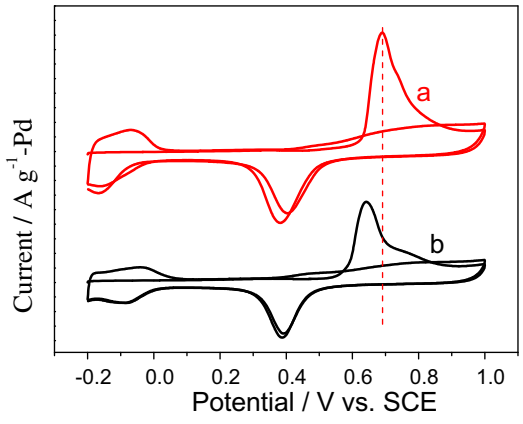

Fig. 5. Cyclic voltammograms of pre-adsorbed CO at (a) Pd/MWCNTs and (b) Pd–P/MWCNTs in N_2-saturated 0.5 M H_2SO_4 solutions at 50 mV s^{-1}.

The electrocatalytic activities of Pd/MWCNTs and Pd–P/MWCNTs catalysts were characterized by cyclic voltammetry. Fig. 6A shows cyclic voltammograms of Pd/MWCNTs and Pd–P/MWCNTs catalysts in the 1 M KOH+1 M CH_3CH_2OH solution at the rate of 50 mV s^{-1}. In the positive scan direction, the onset oxidation potential and the peak potential of ethanol electrooxidation locate at ca. −0.63 V and ca. −0.13 V for all catalysts, respectively. However, it is observed that peak currents of ethanol oxidation are 1821.4 and 2410.6 A g^{-1}-Pd on Pd/MWCNTs and Pd–P/MWCNTs catalysts, showing that the mass activity of Pd–P/MWCNTs catalyst is a factor of 1.3 higher than Pd/MWCNTs catalyst. Long-term stabilities of catalysts were also investigated by

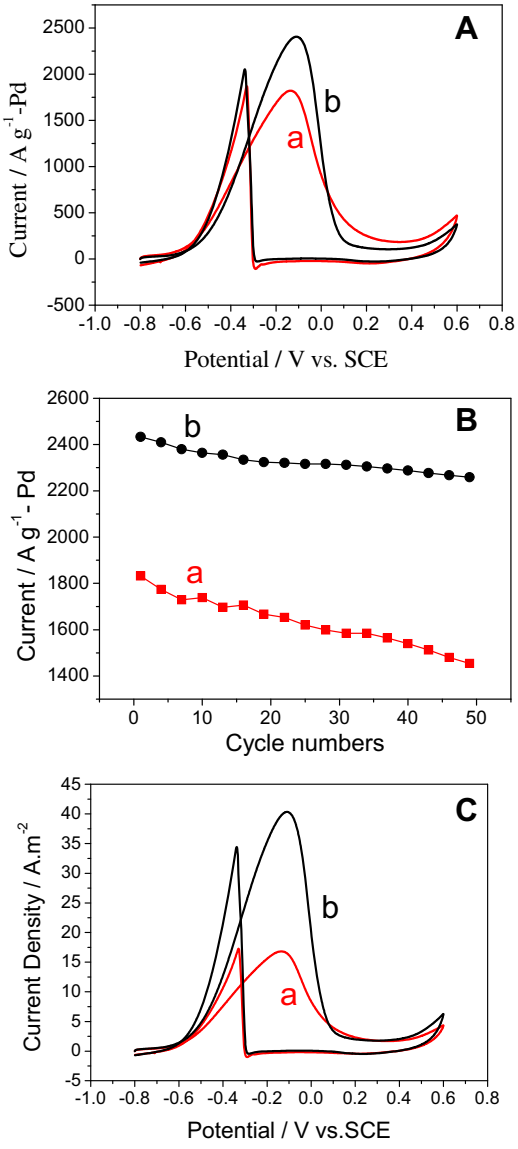

Fig. 6. (A) Cyclic voltammograms and (B) long-term stabilities of (a) Pd/MWCNTs and (b) Pd–P/MWCNTs catalysts in the 1 M KOH + 1 M CH_3CH_2OH solution at the rate of 50 mV s^{-1}. (C) Corresponding cyclic voltammograms normalized using Pd electrochemically active surface area (A m^{-2}-Pd).

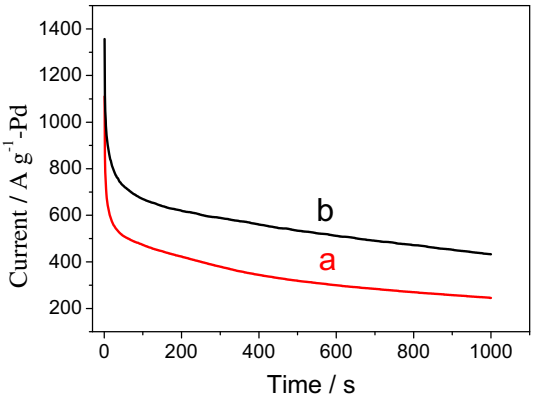

Fig. 7. Chronoamperometric curves of (a) Pd/MWCNTs and (b) Pd–P/MWCNTs catalysts in the 1 M KOH + 1 M CH_3CH_2OH solution at −0.2 V.

continuous cyclic voltammetry measurements (Fig. 6B). As observed, the ethanol oxidation current on Pd–P/MWCNTs catalyst is higher than Pd/MWCNTs catalyst in the whole process, indicating that Pd–P/MWCNTs catalyst has better durability and stability for ethanol electrooxidation than Pd/MWCNTs catalyst. It is well known that the specific activity of catalyst demonstrates the intrinsic activity of the metal nanoparticles. Fig. 6C shows that the peak current density (i.e., the specific activity) of ethanol oxidation on Pd–P/MWCNTs catalyst is about 2.4 times larger than that on Pd/MWCNTs catalyst, illustrating that P can promote the electrocatalytic activity of Pd nanoparticles for ethanol electrooxidation.

The electrochemical stabilities of catalysts were further investigated by chronoamperometric experiments (Fig. 7). It is observed that the ethanol oxidation currents at the Pd/MWCNTs and Pd–P/MWCNTs catalysts at 1000 s are 239.2 and 429.4 A g^{-1} Pd, corresponding to 49.1% and 35.2% of their initial values, respectively. This further confirms that the electrocatalytic mass activity and stability of Pd–P/MWCNTs catalyst are much better than that of Pd/MWCNTs catalyst.

4. Conclusions

In summary, the highly dispersed and ultrafine Pd–P/MWCNTs catalyst can be synthesized by homogeneous precipitation–reduction reaction method. The electrochemical measurements show that the addition of P in Pd nanoparticles can promote the electrocatalytic activity and stability of Pd catalyst for ethanol electrooxidation. The improved activity and stability of Pd–P/MWCNTs catalyst are attributed to following reasons: i) the low hydroxyl surface coverage on Pd–P/MWCNTs, which facilitates the ethanol oxidation kinetics; ii) the abundant O-containing surface species originated from phosphorus oxide, which accelerates the oxidation of CO_{ads} to CO_2 via the so-called bifunctional mechanism.

Acknowledgements

The authors are grateful for the financial support of NSFC (21073094), the United Fund of NSFC and Yunnan Province (U1137602), Natural Science Foundation of Jiangsu Higher Education Institutions of China (10KJB150007), and a project funded by the Priority Academic Program Development of Jiangsu Higher Education Institutions.

References

[1] V. Bambagioni, C. Bianchini, A. Marchionni, J. Filippi, F. Vizza, J. Teddy, P. Serp, M. Zhiani, J. Power Sources 190 (2009) 241–251.
[2] M.M.O. Thotiyl, T.R. Kumar, S. Sampath, J. Phys. Chem. C 114 (2010) 17934–17941.
[3] J.P. Liu, H.H. Zhou, Q.Q. Wang, F.Y. Zeng, Y.F. Kuang, J. Mater. Sci. 47 (2012) 2188–2194.
[4] W.X. Du, K.E. Mackenzie, D.F. Milano, N.A. Deskins, D. Su, X.W. Teng, ACS Catal. 2 (2012) 287–297.
[5] Z.L. Wen, S.D. Yang, Y.Y. Liang, W. He, H. Tong, L.A. Hao, X.G. Zhang, Q.J. Song, Electrochim. Acta 56 (2010) 139–144.
[6] L.H. Jou, J.K. Chang, T.J. Whang, I.W. Sun, J. Electrochem. Soc. 157 (2010) D443–D449.
[7] S.Y. Shen, T.S. Zhao, Q.X. Wu, Int. J. Hydrogen Energy 37 (2012) 575–582.
[8] F.J. Miao, B.R. Tao, Electrochim. Acta 56 (2011) 6709–6714.
[9] F. Ksar, L. Ramos, B. Keita, L. Nadjo, P. Beaunier, H. Remita, Chem. Mater. 21 (2009) 3677–3683.
[10] L.D. Zhu, T.S. Zhao, J.B. Xu, Z.X. Liang, J. Power Sources 187 (2009) 80–84.
[11] J. Bagchi, S.K. Bhattacharya, Trans. Metal. Chem. 32 (2007) 47–55.
[12] J. Bagchi, S.K. Bhattacharya, Trans. Metal. Chem. 33 (2008) 113–120.
[13] Y. Wang, T.S. Nguyen, X.W. Liu, X. Wang, J. Power Sources 195 (2010) 2619–2622.
[14] G. Yang, Y. Chen, Y. Zhou, Y. Tang, T. Lu, Electrochem. Commun. 12 (2010) 492–495.
[15] H.J. Sun, J.F. Xu, G.T. Fu, X.B. Mao, L. Zhang, Y. Chen, Y.M. Zhou, T.H. Lu, Y.W. Tang, Electrochim. Acta 59 (2012) 279–283.
[16] J. Ma, Y.G. Ji, H.J. Sun, Y. Chen, Y.W. Tang, T.H. Lu, J.W. Zheng, Appl. Surf. Sci. 257 (2011) 10483–10488.
[17] P. Li, H. Liu, Y. Ding, Y. Wang, Y. Chen, Y. Zhou, Y. Tang, H. Wei, C. Cai, T. Lu, J. Mater. Chem. 22 (2012) 15370–15378.
[18] Y. Liang, M.N. Zhu, J. Ma, Y.W. Tang, Y. Chen, T.H. Lu, Electrochim. Acta 56 (2011) 4696–4702.
[19] G.J. Zhang, Y.E. Wang, X. Wang, Y. Chen, Y.M. Zhou, Y.W. Tang, L.D. Lu, J.C. Bao, T.H. Lu, Appl. Catal. B Environ. 102 (2011) 614–619.
[20] Y. Chen, Y.M. Zhou, Y.W. Tang, T.H. Lu, J. Power Sources 195 (2010) 4129–4134.
[21] G. Cui, H. Liu, G. Wu, J. Zhao, S. Song, P.K. Shen, J. Phys. Chem. C 112 (2008) 4601–4607.
[22] H. Nakai, T. Homma, I. Komatsu, T. Osaka, J. Phys. Chem. B 105 (2001) 1701–1704.
[23] R. Diegle, N. Sorensen, C. Clayton, M. Helfand, Y. Yu, J. Electrochem. Soc. 135 (1988) 1085–1092.
[24] G. Gutzeit, Plating 47 (1960) 63–70.
[25] P. Hersche, Trans. Ins. Met. Finish 33 (1953) 417–421.
[26] R.M. Lukes, Plating 51 (1964) 969–971.
[27] X. Xue, J. Ge, C. Liu, W. Xing, T. Lu, Electrochem. Commun. 8 (2006) 1280–1286.
[28] X. Xue, J. Ge, T. Tian, C. Liu, W. Xing, T. Lu, J. Power Sources 172 (2007) 560–569.
[29] S. Suzuki, Y. Ohbu, T. Mizukami, Y. Takamori, M. Morishima, H. Daimon, M. Hiratani, J. Electrochem. Soc. 156 (2009) B27–B31.
[30] J.A. Ma, Y.W. Tang, G.X. Yang, Y. Chen, Q. Zhou, T.H. Lu, J.W. Zheng, Appl. Surf. Sci. 257 (2011) 6494–6497.
[31] L.L. Zhang, Y.W. Tang, J.C. Bao, T.H. Lu, C. Li, J. Power Sources 162 (2006) 177–179.
[32] H. Tsunoyama, N. Ichikuni, H. Sakurai, T. Tsukuda, J. Am. Chem. Soc. 131 (2009) 7086–7093.
[33] M. Mason, L. Gerenser, S.T. Lee, Phys. Rev. Lett. 39 (1977) 288–291.
[34] L. Qiu, F. Liu, L. Zhao, W. Yang, J. Yao, Langmuir 22 (2006) 4480–4482.
[35] B. Hammer, J. Norskov, Surf. Sci. 343 (1995) 211–220.
[36] M. Mavrikakis, B. Hammer, J.K. Norskov, Phys. Rev. Lett. 81 (1998) 2819–2822.
[37] F. Lima, J. Zhang, M. Shao, K. Sasaki, M. Vukmirovic, E. Ticianelli, R. Adzic, J. Phys. Chem. C 111 (2007) 404–410.
[38] B. Hammer, Y. Morikawa, J.K. Nørskov, Phys. Rev. Lett. 76 (1996) 2141–2144.
[39] J. Xu, G. Fu, Y. Tang, Y. Zhou, Y. Chen, T. Lu, J. Mater. Chem. 22 (2012) 13585–13590.
[40] H. Liu, A. Manthiram, Energy Environ. Sci. 2 (2009) 124–132.
[41] B.D. Adams, G. Wu, S. Nigro, A. Chen, J. Am. Chem. Soc. 131 (2009) 6930–6931.
[42] D. Wang, H.L. Xin, Y. Yu, H. Wang, E. Rus, D.A. Muller, H.D. Abruna, J. Am. Chem. Soc. 132 (2010) 17664–17666.
[43] C.V. Rao, B. Viswanathan, Electrochim. Acta 55 (2010) 3002–3007.
[44] D. Morales-Acosta, J. Ledesma-Garcia, L.A. Godinez, H. Rodriguez, L. Alvarez-Contreras, L. Arriaga, J. Power Sources 195 (2010) 461–465.
[45] J.Y. Zhao, M.N. Zhu, M. Zheng, Y.W. Tang, Y. Chen, T.H. Lu, Electrochim. Acta 56 (2011) 4930–4936.
[46] X. Wang, Y. Xia, Electrochim. Acta 54 (2009) 7525–7530.
[47] W.J. Zhou, J.Y. Lee, J. Phys. Chem. C 112 (2008) 3789–3793.
[48] J. Jiang, A. Kucernak, J. Electroanal. Chem. 630 (2009) 10–18.